JNeurosci
THE JOURNAL OF NEUROSCIENCE

Research Articles: Behavioral/Cognitive

Individual differences in decision strategy relate to neurochemical excitability and cortical thickness

https://doi.org/10.1523/JNEUROSCI.1086-23.2023

Cite as: J. Neurosci 2023; 10.1523/JNEUROSCI.1086-23.2023

Received: 11 June 2023
Revised: 22 August 2023
Accepted: 26 August 2023

Individual differences in decision strategy relate to neurochemical excitability and cortical thickness

Hannah L. Filmer*[1], Kathleen Loughnan[1], Jennifer X. Seeto[1], Timothy Ballard[1], Shane E. Ehrhardt[1], Thomas Shaw[2,3], Yohan Wards[1], Reuben Rideaux[4,5], Li-Ann Leow[1], David Sewell[1], Paul E. Dux[1]

[1]School of Psychology, The University of Queensland, St Lucia, Australia
[2]School of Information Technology and Electrical Engineering, The University of Queensland, St Lucia, Australia
[3]Centre for Advanced Imaging, The University of Queensland, St Lucia, [4]Queensland Brain Institute, The University of Queensland, St Lucia, Australia
[5]School of Psychology, The University of Sydney, Camperdown, Australia

* Corresponding author
h.l.filmer@gmail.com
Address: McElwain Building, Campbell Road, St Lucia, 4072, Australia

Acknowledgements
This research was supported by Australian Research Council (ARC) Discovery grants (DP180101885, PED; DP210101977 to PED and HLF). HLF and TB were supported by ARC Discovery Early Career Researcher Awards (HLF: DE190100299, TB: DE180101340).

Abstract

The speed-accuracy trade-off (SAT) – whereby faster decisions increase the likelihood of an error – reflects a cognitive strategy humans must engage in during the performance of almost all daily tasks. To date, computational modelling has implicated the latent decision variable of response caution (thresholds) - the amount of evidence required for a decision to be made - in the SAT. Previous imaging has associated frontal regions – notably the left prefrontal cortex and the pre supplementary motor area (preSMA) – with the setting of such caution levels. In addition, causal brain stimulation studies, using transcranial direct stimulation (tDCS), have indicated that while both of these regions are involved in the SAT, their role appears to be dissociable. tDCS efficacy to impact decision-making processes has previously been linked with neurochemical concentrations and cortical thickness of stimulated regions. However, to date, it is unknown if these neurophysiological measures predict individual differences in the SAT, and brain stimulation effects on the SAT. Using ultra-high field (7T) imaging, here we report that instruction-based adjustments in caution are associated with both neurochemical excitability (the balance between GABA+ and glutamate) and cortical thickness across a range of frontal regions in both sexes. In addition, cortical thickness, but not neurochemical concentrations, was associated with the efficacy of left prefrontal and superior medial frontal cortex stimulation to modulate performance. Overall, our findings elucidate key neurophysiological predictors – frontal neural excitation – of individual differences in latent psychological processes and the efficacy of stimulation to modulate these.

Significance Statement

The speed-accuracy trade-off (SAT) - faster decisions increase the likelihood of an error - reflects a cognitive strategy humans must engage in during most daily tasks. The SAT is often investigated by explicitly instructing participants to prioritise speed or accuracy when responding to stimuli. Using ultra-high field (7T) MRI, we found that individual differences in the extent to which participants adjust their decision strategies with instruction related to neurochemical excitability (ratio of GABA+ to glutamate) and cortical thickness in the frontal cortex. Moreover, brain stimulation to the left prefrontal and the superior medial frontal cortices modulated performance, with the efficacy specifically related to cortical thickness. This work sheds new light on the neurophysiological basis of decision strategies and brain stimulation.

Introduction

The faster we make decisions, the more likely we are to make an error. This ubiquitous phenomenon, known as the speed-accuracy trade-off (SAT), reflects a decision strategy humans engage in during the performance of almost all daily tasks, from the simple (e.g., cooking, driving) to the critical (e.g., surgery, military command). In some contexts, it may be more appropriate to prioritise accuracy – for example when driving down a busy road – but under other circumstances, speed may have greater importance – for example if you have a passenger experiencing a medical emergency (and you must get them to a hospital). The cognitive and neural underpinnings of this simple strategic process have been the topic of intense scientific investigation (Heitz, 2014) and the generalisability of the SAT has even been demonstrated in climbing plants as they assess the strength of the supports they coil around (Ceccarini et al., 2020).

To assess the SAT, research has predominantly used simple decision-making paradigms (e.g., discriminating the motion direction of a cloud of dots) with varying task instructions: prioritise speed, prioritise accuracy, or balance the two. Computational modelling (e.g., the linear ballistic accumulator model, LBA; Brown & Heathcote, 2008) has been applied to assess underlying latent process(es) involved in the SAT: Specifically, reaction time and accuracy data can be decomposed into latent decision variables of drift rates (evidence accumulation rates) and response caution (threshold; see Figure 1). The SAT has predominantly been associated with changes in response caution (e.g., Palmer et al., 2005) – whereby speed focused decisions have lower caution than accuracy focused conditions – although drift rates may also play a role (e.g., Sewell & Stallman, 2020).

In terms of the underlying neurophysiology associated with the SAT, imaging studies have implicated activity in, and the structure of, frontal cortices. Specifically, task instruction manipulations of the SAT have been linked to activity in the pre-supplementary motor area (preSMA) and striatum (Forstmann et al., 2008), and left prefrontal cortex (Ivanoff et al., 2008; Vallesi et al., 2012). Studies with patients who have brain tumours have also implicated the left prefrontal (and not right) in the setting of response caution (Campanella et al., 2016). Individual differences analyses have correlated the strength of structural (white matter) connectivity between the preSMA and the striatum to the degree of adjustment to response caution with instruction (Forstmann et al., 2010). This work has been instrumental in developing our understanding of the SAT, however imaging methodology is inherently correlational and previous studies have generally used small sample sizes (e.g., n=9, Forstmann et al., 2010).

Taking a causal approach, we have previously shown that offline cathodal transcranial direct current stimulation (tDCS) applied to the left prefrontal cortex and the superior medial frontal cortex (SMFC, which includes the preSMA) can modulate decision strategies (Filmer et al., 2021): stimulating these two regions modulates response caution, but in opposing directions thus implying different processes/mechanisms of action. However, the efficacy of tDCS to modulate performance varies substantively between individuals (e.g., Wiethoff et al., 2014). This variability has been related to individual differences in underlying

neurophysiology. Specifically, cortical thickness in regions proximal to the targeting electrode (Filmer et al., 2019), and concentrations of neurochemicals – the ratio of the key inhibitory (γ-Aminobutyric acid, GABA) and excitatory (glutamate, Glu) neurochemicals – have been linked to frontal (Filmer, Ehrhardt, Bollmann, et al., 2019) and motor cortex (Stagg et al., 2011) stimulation outcomes.

To date, it is unknown what neurophysiological factors relate to individual differences in decision strategies, or stimulation efficacy to modulate these. We assessed whether the relative concentrations of GABA+ and Glu, and cortical thickness in frontal regions, related to decision strategies and modulations to the SAT via stimulation. Using ultra-high field MRI (7T), magnetic resonance spectroscopy (MRS) was acquired to estimate neurochemical concentrations in the left prefrontal cortex (and visual cortex as a control region), and T1-weighted (T1w) scans to estimate cortical thickness. To preview the results, decision strategy adjustment related to cortical thickness across a range of frontal areas and the ratio of GABA+ to Glu in left prefrontal cortex. Moreover, the efficacy of left prefrontal and SMFC stimulation to modulate decision strategies related to cortical thickness.

Method

Experimental design

The experiment was based on an approach previously employed by Filmer et al. (2021). Participants who had previously undergone neuroimaging at 7T were recruited, with all subsequent testing pre-registered (https://osf.io/b47dm/). Each participant completed three counterbalanced stimulation sessions in which they received a different form of cathodal stimulation: stimulation to the SMFC, stimulation to the left prefrontal cortex, and a sham condition. The task involved participants discriminating motion direction (left or right) from a random dot motion stimulus, where they were instructed, across blocks, to prioritise speed, accuracy, or balance the two. Computational modelling (via the LBA, Brown & Heathcote, 2008) was applied to estimate latent decision-making variables (drift rates and response caution).

Participants

As per our pre-registration, we aimed to recruit participants until one of the following occurred: we obtained data from 78 participants, our stopping date was reached, or we exhausted our participant pool. The latter two both occurred, with 38 participants tested in total (14 male, 24 female, mean age = 24, SD = 4.85). The subjects were screened in advance to ensure they could safely receive tDCS. In addition, any subjects with performance close to floor (< 60%) or ceiling (> 90%) for any of the three strategy conditions were excluded from the analysis. As a slight deviation from our preregistration, this was done on a session basis, so if performance met exclusion criteria for one session, only that session's data were removed. In the case that performance in the sham condition was affected, all data were removed as the sham session acted as baseline. This approach was taken to maximise data inclusion. In total, data were completely removed for two participants (one for

performance < 60%, one for performance > 90%), active prefrontal data were removed for one further subject (performance < 60%), and active SMFC data were removed for four subjects (one for performance < 60%, three for performance > 90%).

Task

A random dot motion (RDM) task with varying speed-accuracy condition instructions was employed. In each trial, participants viewed a display with a fixation dot (1000ms), followed by the random dot display containing 200 dots (500ms; see Figure 2). The dot display was presented in a circular area with a diameter of 3.4° visual angle and the dots moved at a rate of 0.46° visual angle/second. The display contained a portion of dots (75%) moving coherently either to the top left or right of the screen, while the rest moved randomly. In each trial, subjects discriminated the direction of coherent motion. Each session started with a short practice block, followed by a thresholding procedure. The thresholding procedure used a QUEST staircase (Watson & Pelli, 1983) to achieve ~ 70% accuracy via varying the degree of offset from the vertex for the motion. Three overlapping staircases were used, running for a total of 90 trials. A short check then occurred (20 trials), and if performance was < 60% or > 90%, the staircase procedure was re-run. Directly after thresholding, the subjects completed a short practice of the main task with one short (10 trial) block for each instruction condition: emphasise accuracy, emphasise speed, or balance the two.

Next, subjects received stimulation (see details below). The main task then started within 2 minutes of the cessation of stimulation. This phase of the experiment consisted of 36 blocks (12 per instruction condition). The block types were pseudo-randomly intermixed, controlling for the direction and distance of instruction shifts, and ensuring the different block types occurred equally often across every 6 blocks of the experiment. The length of each block averaged 25 trials (minimum of 20, maximum of 30, with a standard deviation of 3; approx. 300 trials per response strategy per session). A 30 second break was given every 6 blocks. The total duration of the main task was 35 minutes.

tDCS

The tDCS procedure was identical to Filmer et al. (2021), wherein two different brain regions were targeted using the 10-20 EEG system: the SMFC (1 cm posterior to the Fz electrode) and the left PFC (1 cm posterior to the F3 electrode). In all sessions, the target electrode was the cathode, and the reference/return (anode) electrode was placed over the right orbitofrontal area (just above the eyebrow). The electrodes were 5 x 5 cm saline-soaked sponges, with stimulation administered at 0.7mA, a stimulation density that is common across the literature (Filmer et al., 2013; Filmer et al., 2021; Nitsche & Paulus, 2000; Stagg et al., 2013).

Subjects received three different types of stimulation across the sessions: active stimulation to the left prefrontal cortex, active stimulation to the SMFC, or sham (placebo) stimulation. The location of the electrodes for the sham condition was controlled across subjects. Specifically, odd subject numbers received sham with the

prefrontal electrode montage, and even subject numbers the SMFC electrode montage. The order of the sessions was counterbalanced across subjects. Subjects were blinded for all sessions. Due to the design, the experimenters were blinded for the sham session and one of the active stimulation sessions. That is, for those subjects receiving sham stimulation with the prefrontal montage, the experimenter was blinded for the active prefrontal and sham conditions, but not for the SMFC condition. We probed subjects, at the end of the final session, to ascertain if they could discriminate the stimulation types.

For active stimulation, the current ramped up for 30 seconds, held constant for 19 minutes, then ramped down for 30 seconds. For the sham stimulation, the current ramped down after 15 seconds and administered small testing pulses to provide an online measure of impendence for the experimenter, continuing sensation for the participant, and thus give the illusion that the stimulation continues to run.

MRI

Across three imaging sessions, MR images were acquired on a 7 T whole-body research scanner (Siemens Healthcare, Erlangen, Germany), with maximum gradient strength of 70 mT/m and a slew rate of 200 mT/m/s and a 7 T Tx/32 channel Rx head array (Nova Medical, Wilmington, MA, USA). A total of 178 participants were scanned three times (in separate sessions) using an anatomical whole-brain T1w scan using a prototype MP2RAGE sequence (WIP 900; Marques et al., 2010; O'Brien et al., 2014) at 0.75 mm isotropic voxel size (TR/TE/TIs = 4300 ms / 2.5 ms / 840 ms, 2370 ms, TA = 6:54) as part of another project. A total of three participants did not have usable data (likely due to movement) and were excluded from the cortical thickness analyses.

T1w images were segmented using Advanced Normalisation Tools (ANTs) version >=2.2.3. We first constructed a population-specific template (of 50 participants) using antsMultivariateTemplateConstruction2.sh and 20 iterations to achieve good convergence. The template was then labelled using the antsCookTemplatePriors script to construct our own tissue priors for all subsequent processing. Following this atlas construction, we used the antsLongitudinalCorticalThickness.sh script with default parameters for cortical thickness and white and grey matter labelling of each subject at each time-point. Finally, we employed Joint Label Fusion (JLF) with a subset of the Mindboggle-101 (Klein et al., 2017; Klein & Tourville, 2012) label priors to label each participants' DKT-31 regions (Klein & Tourville, 2012) at each time-point. The ROIs included in this study were frontal regions across the two hemispheres (see Figure 4) as we anticipated they could be influenced by stimulation and involved in the SAT. Cortical thickness estimates and volume for these regions of interest (ROI) were calculated using ANTs including mean, min, max, and SD cortical thickness values, surface area, and volume for the given ROIs. Our analyses focused upon cortical thickness, and visual inspection of the cortical thickness images were completed. As each participant was scanned three times, we took the median cortical thickness values for each participant. The final data were checked for outliers (values > 3 SD from the mean), and none were found.

MRS

Using the same scanner as above, anatomical T1-weighted images were acquired to allow for MRS voxel placement (MP2-RAGE sequence: TR = 4300ms, TE = 3.38ms). One voxel was placed over the left prefrontal cortex (40 x 26 x 26 mm), positioned on a slice 1.5mm above the superior margin of the lateral ventricles with the centre one third of the total anterior/posterior distance and halfway between the mid-line and the left lateral border (see Figure 5). The other voxel was positioned centrally across the bilateral midline, above and aligned to the calcarine fissure. To detect GABA+, a MEGA-sLASER sequence (Andreychenko et al., 2012) was used (key parameters: TE = 74ms, TR = 7800ms, bandwidth = 4000 Hz, 64 transients of 4096 data points, 2 water-unsuppressed transients also acquired, and a 23.6ms Gaussian editing pulse was applied at 1.90 (ON) and 7.46 (OFF) ppm). Water suppression occurred via variable power with optimised relaxation delays (VAPOUR, Tkáč & Gruetter, 2005). To detect Glu, a sLASER sequence (Scheenen et al., 2008) was used (key parameters: TE = 42ms, TR = 7790 ms, spectral width = 4000 Hz, 32 transients of 4096 data points acquired). In addition, a single inversion recovery metabolite nulling in sLASER (TI = 1135 ms) was performed in two subjects to estimate, and in the analyses constrain, metabolite quantification (Cudalbu et al., 2021). In quick succession, automated shimming with 3D GRE brain followed by FAST(EST)MAP shimming were run. The acquisition window for MRS sequences was 1000ms, however we only used the first 250ms of the data for each acquisition as there was no signal in the free induction decay after this time. All MRS data were analysed from the Siemens TWIX format.

We used the same procedures for spectral pre-processing and quantification as Rideaux et al. (2022). Briefly, all edited (MEGA) sub-spectra were 3-Hz exponentially line-broadened and zero-filled to a spectral resolution of 0.061 Hz/point. For all data, frequency and phase parameter estimates were obtained by modelling the total creatine (creatine and phosphocreatine) signal, then these parameters were used to align sub-spectra to a common frequency and phase, as previous work has shown this is the most effective method of alignment for GABA+ quantification (Rideaux et al., 2021). For edited data, the average ON and OFF spectra were subtracted to produce the edited spectrum, from which GABA+ (3 ppm) signal intensity was modelled using a Lorentzian. Similarly, water signal intensity was determined by fitting a Lorentzian model to the average water-unsuppressed spectra at 4.7 ppm. For unedited data, glutamate and water signal intensity were quantified using LCModel. GABA and glutamate concentrations were calculated as the area and the peak of the fitted peak, respectively, and expressed in institutional units (i.u.) using the unsuppressed water signal as an internal concentration reference. We further applied a tissue-correction method that accounts for differences in relaxation times across the tissue types within a voxel (Gasparovic et al., 2006).

It should be noted that the MRI/MRS data were collected for a separate project, and there was ~1 year in between imaging and the SAT/tDCS sessions. MRI/MRS measures have been shown to be stable over time (e.g. Greenhouse et al., 2016; Near et al., 2014): thus, our MRI/MRS measures remain robust and valid.

Statistical analyses

Computational modelling. Drift rates and response thresholds were estimated using the linear ballistic accumulator (LBA) model within a hierarchical Bayesian framework, which captures individual differences in process components while also providing information about each quantity at the group level. The model was identical to the one specified by Filmer et al. (2021) except that the mean drift rate for the incorrect response alternative was fixed across experimental conditions. This was done to enable a more reliable measure of discriminability and caution (see Evans, 2020).

Discriminability was indexed as the mean drift rate for the correct response alternative. Given that the mean drift rate for the incorrect response was fixed across conditions, changes in mean drift rate for the correct response across conditions also reflected changes in the difference in the mean drift rates between the correct and incorrect response alternatives. Response caution was indexed as the difference between the response threshold and the maximum starting point of evidence accumulation. Discriminability and response caution were allowed to vary across experimental conditions, while non-decision time, the maximum start point of evidence, and the sum of the correct and error drift rates were fixed across conditions. To ensure model identifiability, the standard deviation of both drift rates was fixed to one in all conditions. We used 95% credible intervals to make inferences about group-level effects.

Individual differences analyses. Regression analyses were conducted to assess for associations between individual differences in the latent decision process components of the SAT and in the efficacy of tDCS to modulate these. These analyses utilised response caution and discriminability measures derived from the LBA model. The following variables were calculated: 1. The change in caution with instruction; 2. The change in discriminability with instruction; 3. Overall caution; 4. Overall discriminability. The two change measures were calculated by subtracting the value in the speed-focused condition from the value in the accuracy-focused condition, and the two overall conditions were the average across instruction. These variables were calculated for each session, and then active stimulation was compared to sham (e.g., the change in caution was subtracted for active vs sham sessions to derive the extent to which stimulation increased the change in caution) and used as the dependent variables in the analyses reported below. Independent variables were the concentrations of neurochemicals, and cortical thickness for frontal regions. For cortical thickness, we had a relatively large number of brain regions across the frontal cortex (a total of 12 regions, see Figure 4) which made initial Bayesian regressions computationally intensive and thus impractical to run. Thus, we initially conducted linear backward regressions as a form of variable selection (stepping method criteria based on p values, entry of 0.05 and removal 0.1). The variables identified from this were then included in a Bayesian Linear Regression. All regression analyses were completed in JASP (JASP Team, 2017), and included order of session completion in the null model to account for the order of session completion. The regression analyses with cortical thickness also included total brain volume in the null model. The Bayes factors (BF) were interpreted as follows (either in favour of the alternate – BF_{10} – or null – BF_{01} – hypotheses): 1-1.3 as indeterminant, 1.3-3 as weak evidence, 3-10 as moderate evidence, and >10 as strong evidence.

Results

Group level effects

Manipulation check. From the sham sessions, we found the instruction manipulation successfully modulated both response caution and discriminability (see Figure 6). Specifically, accuracy-focused instruction resulted in more cautious responses than mixed [0.098 0.151] or speeded [0.405 0.456], and mixed was also more cautious than speeded [0.283 0.33]. Speeded instruction resulted in lower discriminability than mixed [0.027 0.123] or accuracy [0.022 0.12], and mixed and accuracy were not credibly different [-0.052 0.043].

Stimulation effects on response caution. Overall, we replicated our previous findings (Filmer et al., 2021) showing that stimulation to the SMFC reduces response caution relative to sham [0.148 0.239] (see Figure 7). However, this effect did not interact with instruction (CIs for differences between instruction conditions all contained 0). We had anticipated that stimulation to the prefrontal cortex would increase caution, but in fact found the opposite [0.072 0.147], although the decrease was to a lesser extent than stimulation to the SMFC [0.035 0.134]. The effect of prefrontal stimulation interacted with instruction, such that the effect of stimulation was greater for accuracy compared with speeded instruction [0.01 0.157], with no other comparisons credible (all CIs contained 0).

Stimulation effects on discriminability. Our pre-registered hypotheses focused upon stimulation modulating caution. Nonetheless, we had previously found (and thus anticipated) that stimulation to the SMFC increased discriminability. Here, however, stimulating the SMFC did not credibly modulate discriminability compared to sham [-0.086 0.017], and there were no interactions between the instruction conditions (all intervals contained 0). Stimulating the prefrontal cortex modulated discriminability relative to sham stimulation [0.019 0.102], although there was no difference between prefrontal and SMFC sessions [-0.084 0.031]. For prefrontal stimulation (relative to sham) there were no differences between instruction conditions (all intervals contained 0). As the two active stimulation conditions were not distinct, overall, there is little evidence to support stimulation modulating discriminability.

Neurophysiological correlates of the SAT

Neurochemicals. For the sham stimulation sessions, the amount of adjustment in thresholds with instructions correlated with neurochemical concentrations (see Figure 8). Specifically, adjustment in threshold with task instruction related to E/I balance in the left prefrontal cortex (BF_{10} = 4.932, R^2 = 0.2) with lower E/I ratio (more excitatory neurochemical balance) associated with greater response caution adjustment. No relationships were evident with neurochemical concentrations in the visual cortex (BF_{10} < 0.6 for all). Average caution, which could be thought of as how cautious overall an individual was in their response, was not related to E/I in either region of interest (PFC, BF_{10} < 0.56 for all; VC, BF_{10} < 0.9 for all). E/I was also not related to adjustment in discriminability for either region of interest (BF_{10} < 0.7 for all). There was only weak evidence for a relationship between mean discriminability and glutamate in the left prefrontal cortex (BF_{10} = 1.99, R^2 = 0.132), and no evidence

for any relationship for visual cortex (BF_{10} < 0.93 for all). Thus, overall, E/I balance was predominantly related to adjustments in thresholds with task instruction.

Cortical thickness. Overall, baseline cortical thickness in left and right frontal regions related to both caution and discriminability. Specifically, there was moderate evidence that the amount of adjustment in caution related to left and right rostral middle frontal, and left caudal middle frontal, gyri (BF_{10} = 4.631, R^2 = 0.427; see Figure 9) with thicker cortex in the left hemisphere leading to less, and the right hemisphere more, adjustment in caution. There was also strong evidence that the average caution related to right rostral middle frontal and left pars triangularis gyri (BF_{10} = 14.411, R^2 = 0.419), with thicker cortex in the left pars triangularis, and thinner cortex in the right rostral middle frontal gyrus, relating to less overall caution. Thus, there is a pattern for an opposing relationship between left and right hemisphere cortical thickness and adjustments in, and overall level of, thresholds. Moreover, the middle frontal gyrus (in both hemispheres) appears to be an important region relating to response caution. This is in line with the previous literature: the middle frontal gyrus has been implicated in previous imaging studies (Ivanoff et al., 2008) and was a key target in previous tDCS studies (Filmer et al., 2021, 2023). But, further, it appears that there is some differing role for the two hemispheres.

For discriminability, there was moderate evidence that the adjustment with instruction related to a broad range of frontal regions across both hemispheres. Specifically, more adjustment in discriminability was associated with thicker cortex in right pars opercularis, left precentral and right rostral middle frontal gyri, and thinner cortex in left rostral middle frontal and right precentral gyri (BF_{10} = 5.299, R^2 = 0.48). There was only weak evidence for average discriminability relating to cortical thickness (the left caudal middle frontal gyrus; BF_{10} = 1.52, R^2 = 0.345).

Neurophysiological correlates of prefrontal stimulation efficacy

Neurochemicals. There was little support for neurochemical concentrations relating to the effect of prefrontal stimulation on thresholds or drift rates. There was indeterminate/weak evidence relating stimulation efficacy to modulate the adjustment of thresholds to E/I (BF_{10} = 1.384) and relating stimulation efficacy to modulate average discriminability to glutamate (BF_{10} = 1.428), and all other analyses were indeterminate/in favour of the null (BF_{10} < 0.5 for all).

Cortical thickness. The efficacy of stimulation to the prefrontal cortex (relative to sham) to modulate adjustments in discriminability and the overall level of caution were strongly related to cortical thickness across a range of frontal regions (Table 1). The regions relating to stimulation effects on discriminability and caution were distinct, implying some difference in sources of variability in the efficacy of stimulation to modulate these two processes. Overall, the regions relating to stimulation efficacy included both areas likely to be affected by stimulation (see the current modelling in Figure 3) such as the left rostral and superior frontal gyri, and areas that show relatively less overlap with induced current from stimulation (e.g., right precentral), implying potential direct and indirect relationships between cortical thickness and stimulation outcomes. One possibility is that the areas not likely to be directly affected by stimulation could influence outcomes due to network-level effects of the stimulation that spread beyond target regions.

Neurophysiological correlates of SMFC stimulation efficacy

Neurochemicals. There was no evidence in favour of a relationship between the efficacy of stimulation to SMFC to modulate thresholds or discriminability (in terms of adjustments with instruction, or averages) and neurochemical concentrations (all $BF_{10} < 1.05$).

Cortical thickness. Modulations in the adjustment of caution and discriminability, and in overall level of caution, with stimulation (relative to sham) were associated with a broad range of frontal regions (see Table 1). There was substantial overlap in these regions between caution and discriminability effects, implying the source of variability for SMFC stimulation efficacy was consistent across latent decision variables. Again, the regions relating to stimulation efficacy included both areas likely to be affected by stimulation (see the current modelling in Figure 3) – such as right pars opercularis, pars triangularis, rostral middle frontal, and left caudal middle frontal gyri – and areas that do not largely overlap with induced current from stimulation (e.g., left pars opercularis, precentral, and rostral middle frontal gyri).

Blinding efficacy

At the end of the final session, participants were informed one of the three tDCS sessions involved a sham stimulation. We then asked participants to guess which session they received sham. Overall, there was a correct guess rate of 42%, which showed moderate evidence in favour of the null ($BF_{01} = 3.2$) – i.e., participants could not correctly distinguish active from sham stimulation.

Table 1: Winning regression models relating modulations to caution and discriminability with stimulation (relative to sham) with cortical thickness in frontal regions. * = moderate evidence, ** = strong evidence. + indicates a positive relationship between modulations to behaviour with stimulation and cortical thickness, - indicates a negative relationship.

Stimulated region	Behavioural effect	Cortical thickness regions	BF_{10}	R^2
Prefrontal cortex	Adjustment in Caution	Right pars opercularis (-) and left caudal middle frontal (+) gyri	2.26	0.28
	Adjustment in Discriminability	Left rostral middle frontal (+), right precentral (+), right pars opercularis (-), and left superior frontal (-) gyri	**19.47***	**0.54**
	Average Caution	Left caudal middle frontal (+), left pars triangularis (+), right rostral middle frontal (-) gyri	**175.96****	**0.64**
	Average Discriminability	NA	< 0.75 for all	NA
SMFC	Adjustment in Caution	Bilateral pars opercularis (-), left caudal middle frontal (+), left precentral (+), right pars triangularis (+), and right superior frontal (-) gyri	**15.35****	**0.68**
	Adjustment in Discriminability	Bilateral pars opercularis (-), left caudal middle frontal (+), left precentral (+), right pars triangularis (+), and right superior frontal (-) gyri	**58.46****	**0.77**
	Average Caution	Right pars opercularis (-) and triangularis (+), left precentral (+), left caudal middle frontal (+), left rostral middle frontal (-), and left superior frontal (-) gyri	**6.71***	**0.65**
	Average Discriminability	Right pars opercularis (-) and precentral gyri (+)	2.34	0.33

Discussion

We assessed neurophysiological factors that predict individual differences in decision strategies, and the efficacy of tDCS in modulating these factors. Using a behavioural paradigm where strategy was adjusted via task instruction (emphasise speed, accuracy, or balance the two), we partially replicated previous studies from our lab (Filmer et al., 2021, 2023). Specifically, we again found that stimulation to the SMFC with cathodal tDCS decreased the latent decision process of response caution relative to both sham and left prefrontal stimulation. However, we did not find that stimulation to the left prefrontal increased caution as we anticipated. Of import, performance at the SAT task was related to cortical thickness and neurochemical concentrations in the absence of active stimulation. Furthermore, cortical thickness but not neurochemical concentration was related to the efficacy of tDCS to modulate SAT performance, for both prefrontal and SMFC stimulation.

The study included two separate active stimulation conditions (in addition to sham stimulation), meaning it is unlikely the findings were due to something generic and/or driven by the location of the reference/return electrode. The design was also partially double blind (one active vs sham double blind for each participant), with participants unable to reliably guess which of the three sessions was sham. The sample size was smaller than the initial design (consisting of 34 participants), and there have recently been concerns raised about using relatively small sample sizes in brain-behaviour association studies where small effect sizes are likely (e.g. Marek et al., 2022). However, these criticisms predominantly relate to studies using broader/more general measures of personality, psychopathology, behaviour and cognition (e.g. personality traits assessed via pen and paper tests; NIH Toolbox assessing general cognitive ability). Here, the research question was focused on a highly studied and specific cognitive phenomenon – the SAT – and each participant contributed a large number of trials (~ 2700) to the analyses, resulting in individual participant measures that were relatively precise (see Gratton et al., 2022). Further, the data were analysed using computational modelling to parse performance into latent decision variables. We have also coupled these more precise measures with a brain stimulation intervention, the use of Bayesian statistics, and ultra-high field (7T) neuroimaging giving high resolution for cortical thickness and spectral measures of neurochemical estimates. Thus, collectively, the study was powered to detect behavioral effect sizes and correlations typically seen in similar studies combining MRI, MRS and brain stimulation (e.g. Filmer et al., 2019) and included the most precise behavioural and neuroimaging measures possible. Nevertheless, given the current questions regarding replicating brain-behaviour associations, and that the true effect sizes are unknown, further research will be welcome to corroborate our findings.

The group level results did not fully replicate our previous findings, despite the results having been demonstrated twice before in other studies (Filmer et al., 2021, 2023). Specifically, we did not see the anticipated increase in response caution with tDCS to left prefrontal cortex. More broadly, the use of tDCS has been criticised due to reports of poor replicability (Horvath et al., 2014), and high inter- and intra-individual differences in efficacy (e.g. Chew et al., 2015; Dyke et al., 2016; Wörsching et al., 2017). Indeed, the study reported here aimed to shed light on the

individual differences in stimulation efficacy (also, see Filmer et al., 2020 for a discussion of the fields critique). It is worth noting that the study design was changed from our previous work. For example, the present study was changed to be fully within subjects, with each participant completing three (as opposed to two) experimental sessions with the task. This could have led to increased practice effects, weakening the findings. Also, we found substantial correlations between the effect of prefrontal stimulation and cortical thickness, showing there is a relationship here between the SAT and prefrontal stimulation. It is important to note that despite the lack of replication for the prefrontal cortex we did see a consistent effect from SMFC stimulation, for what is now the third time (Filmer et al., 2021, 2023).

Our data provide a novel insight into the SAT. We are the first to show that neurochemical E/I balance is related to adjustments in caution with instruction. Specifically, individuals who show more of an adjustment in caution with instruction had greater neurochemical excitation in the left prefrontal cortex. Adjustments in, and overall levels of, caution were also linked to cortical thickness in both left and right frontal regions. A clear pattern emerged where thicker cortex in the left, and thinner in right, was associated with less adjustment, and lower overall levels, of caution. A less clear pattern, involving a broader range of regions, was apparent for adjustments in discriminability.

Stimulation efficacy was not related to neurochemical concentrations, in contrast to findings considering stimulation effects on other performance measures such as response selection (Filmer, Ehrhardt, Bollmann, et al., 2019). It is possible the age of the MRS data reduced sensitivity for a possible relationship, although given previous findings relating to the stability of MRS (Greenhouse et al., 2016; Near et al., 2014), and the presence of a relationship with the SAT reported here, this seems unlikely. This implies that tDCS protocols to the frontal cortex can have differing underlying relationships with baseline neurophysiology depending upon the targeted cognitive process. It is also possible that different neurochemicals could play a role in stimulation efficacy, for example, noradrenaline and dopamine, both not measurable with MRS, have been implicated in effects of tDCS on neuroplasticity (Kuo et al., 2017; Nitsche et al., 2006) and the efficacy of tDCS to modulate the SAT (Leow et al., 2023).

Strong relationships were evident, however, between cortical thickness and stimulation efficacy (see also Filmer, Ehrhardt, Shaw, et al., 2019). Overall, a broad range of regions spanning both left and right hemispheres were found to be related. For SMFC stimulation, these regions largely overlapped between the different performance measures (adjustments in caution and discriminability, and overall level of caution). For left prefrontal stimulation, cortical regions relating to performance (adjustments in discriminability and average caution) showed less overlap, suggesting a potential difference in how these two effects were modulated. It is possible that stimulation efficacy relates to cortical thickness due to an influence on current flow. Thicker/thinner cortex could affect the dispersal of the current and thus the influence of stimulation on performance. Alternatively, it may be that cortical thickness relates to cognitive performance and the effect of stimulation on these underlying processes. These two are also not mutually exclusive, and could in

combination explain the data reported here. Given that cortical thickness was found to relate to variability in SAT performance in the absence of stimulation (for the sham sessions only), it does appear that thickness is related to the SAT in some manner. Indeed, there was some overlap between the regions found to relate to adjustments in caution without stimulation, and regions relating to stimulation efficacy. In particular, the left caudal middle frontal gyrus was related to SAT performance in the absence of stimulation, and to tDCS efficacy. This is in line with both the current modelling showing induced electric fields in this region (see Figure 3), and also previous imaging work into the SAT (e.g., Ivanoff et al., 2008). Further work may look to distinguish between the possible contributions of cortical thickness to current dispersal and cognitive performance.

In summary, the work reported here gives unique insights into the neurophysiological variables relating to individual differences in SAT performance and stimulation efficacy. Given both the ubiquity of the SAT in everyday life, and the critique of tDCS for the individual variability in responsiveness (see Filmer et al., 2020), this work helps to elucidate the key mechanisms involved in both. As well as furthering understanding, the findings highlight how we may predict both an individual's SAT performance and how effective stimulation may be for modulating decision strategies. Indeed, in the future this could lead to individually tailored interventions to optimize performance.

References

Andreychenko, A., Boer, V. O., Arteaga de Castro, C. S., Luijten, P. R., & Klomp, D. W. J. (2012). Efficient spectral editing at 7 T: GABA detection with MEGA-sLASER. *Magnetic Resonance in Medicine*, *68*(4), 1018–1025. https://doi.org/10.1002/mrm.24131

Brown, S. D., & Heathcote, A. (2008). The simplest complete model of choice response time: linear ballistic accumulation. *Cognitive Psychology*, *57*(3), 153–178.

Campanella, F., Skrap, M., & Vallesi, A. (2016). Speed-accuracy strategy regulations in prefrontal tumor patients. *Neuropsychologia*, *82*, 1–10. https://doi.org/https://doi.org/10.1016/j.neuropsychologia.2016.01.008

Ceccarini, F., Guerra, S., Peressotti, A., Peressotti, F., Bulgheroni, M., Baccinelli, W., Bonato, B., & Castiello, U. (2020). Speed–accuracy trade-off in plants. *Psychonomic Bulletin & Review*, *27*(5), 966–973. https://doi.org/10.3758/s13423-020-01753-4

Chew, T., Ho, K.-A., & Loo, C. K. (2015). Inter- and Intra-individual Variability in Response to Transcranial Direct Current Stimulation (tDCS) at Varying Current Intensities. *Brain Stimulation*, *8*(6), 1130–1137. https://doi.org/https://doi.org/10.1016/j.brs.2015.07.031

Cudalbu, C., Behar, K. L., Bhattacharyya, P. K., Bogner, W., Borbath, T., de Graaf, R. A., Gruetter, R., Henning, A., Juchem, C., Kreis, R., Lee, P., Lei, H., Marjańska, M., Mekle, R., Murali-Manohar, S., Považan, M., Rackayová, V.,

Simicic, D., Slotboom, J., … Mlynárik, V. (2021). Contribution of macromolecules to brain (1) H MR spectra: Experts' consensus recommendations. *NMR in Biomedicine*, *34*(5), e4393. https://doi.org/10.1002/nbm.4393

Dyke, K., Kim, S., Jackson, G. M., & Jackson, S. R. (2016). Intra-Subject Consistency and Reliability of Response Following 2 mA Transcranial Direct Current Stimulation. *Brain Stimulation*, *9*(6), 819–825. https://doi.org/10.1016/j.brs.2016.06.052

Filmer, H.L., Ehrhardt, S. E., Bollmann, S., Mattingley, J. B., & Dux, P. E. (2019). Accounting for individual differences in the response to tDCS with baseline levels of neurochemical excitability. *Cortex*, *115*. https://doi.org/10.1016/j.cortex.2019.02.012

Filmer, H.L., Ehrhardt, S. E., Shaw, T. B., Mattingley, J. B., & Dux, P. E. (2019). The efficacy of transcranial direct current stimulation to prefrontal areas is related to underlying cortical morphology. *NeuroImage*, *196*. https://doi.org/10.1016/j.neuroimage.2019.04.026

Filmer, H.L., Mattingley, J. B., & Dux, P. E. (2020). Modulating brain activity and behaviour with tDCS: Rumours of its death have been greatly exaggerated. *Cortex*, *123*. https://doi.org/10.1016/j.cortex.2019.10.006

Filmer, H.L., Mattingley, J. B., Marois, R., & Dux, P. E. (2013). Disrupting prefrontal cortex prevents performance gains from sensory-motor training. *Journal of Neuroscience*, *33*(47). https://doi.org/10.1523/JNEUROSCI.2019-13.2013

Filmer, Hannah L., Ballard, T., Amarasekera, K. D. R., Sewell, D. K., & Dux, P. E. (2023). The causal role of the prefrontal and superior medial frontal cortices in the incidental manipulation of decision strategies. *Neuropsychologia*, *179*, 108466. https://doi.org/10.1016/J.NEUROPSYCHOLOGIA.2022.108466

Filmer, Hannah L., Ballard, T., Sewell, D. K., & Dux, P. E. (2021). Causal evidence for dissociable roles of the prefrontal and superior medial frontal cortices in decision strategies. *Journal of Experimental Psychology: Human Perception and Performance*, *47*(4), 518–528. https://doi.org/10.1037/xhp0000896

Filmer, Hannah L., Ehrhardt, S. E., Shaw, T. B., Mattingley, J. B., & Dux, P. E. (2019). The efficacy of transcranial direct current stimulation to prefrontal areas is related to underlying cortical morphology. *NeuroImage*, *196*, 41–48. https://doi.org/10.1016/J.NEUROIMAGE.2019.04.026

Filmer, Hannah L, Ehrhardt, S., Bollmann, S., Mattingley, J. B., & Dux, P. E. (2019). Accounting for individual differences in the response to tDCS with baseline levels of neurochemical excitability. *Cortex*. https://doi.org/10.1016/j.cortex.2019.02.012

Forstmann, B. U., Anwander, A., Schäfer, A., Neumann, J., Brown, S., Wagenmakers, E. J., Bogacz, R., & Turner, R. (2010). Cortico-striatal connections predict control over speed and accuracy in perceptual decision making. *Proceedings of the National Academy of Sciences of the United States of America*, *107*(36), 15916–15920. https://doi.org/10.1073/pnas.1004932107

Forstmann, B. U., Dutilh, G., Brown, S., Neumann, J., Von Cramon, D. Y.,

Ridderinkhof, K. R., & Wagenmakers, E. J. (2008). Striatum and pre-SMA facilitate decision-making under time pressure. *Proceedings of the National Academy of Sciences of the United States of America*, *105*(45), 17538–17542. https://doi.org/10.1073/pnas.0805903105

Gasparovic, C., Song, T., Devier, D., Bockholt, H. J., Caprihan, A., Mullins, P. G., Posse, S., Jung, R. E., & Morrison, L. A. (2006). Use of tissue water as a concentration reference for proton spectroscopic imaging. *Magnetic Resonance in Medicine: An Official Journal of the International Society for Magnetic Resonance in Medicine*, *55*(6), 1219–1226.

Gratton, C., Nelson, S. M., & Gordon, E. M. (2022). Brain-behavior correlations: Two paths toward reliability. *Neuron*, *110*(9), 1446–1449. https://doi.org/https://doi.org/10.1016/j.neuron.2022.04.018

Greenhouse, I., Noah, S., Maddock, R. J., & Ivry, R. B. (2016). Individual differences in GABA content are reliable but are not uniform across the human cortex. *Neuroimage*, *139*, 1–7. https://doi.org/10.1016/j.neuroimage.2016.06.007

Heitz, R. P. (2014). The speed-accuracy tradeoff: History, physiology, methodology, and behavior. In *Frontiers in Neuroscience* (Vol. 8, Issue 8 JUN, p. 150). Frontiers Research Foundation. https://doi.org/10.3389/fnins.2014.00150

Horvath, J. C., Carter, O., & Forte, J. D. (2014). Transcranial direct current stimulation: five important issues we aren't discussing (but probably should be). *Frontiers in Systems Neuroscience*, *8*, 2. https://doi.org/10.3389/fnsys.2014.00002

Ivanoff, J., Branning, P., & Marois, R. (2008). fMRI Evidence for a Dual Process Account of the Speed-Accuracy Tradeoff in Decision-Making. *PLoS ONE*, *3*(7), e2635. https://doi.org/10.1371/journal.pone.0002635

Klein, A., Ghosh, S. S., Bao, F. S., Giard, J., Häme, Y., Stavsky, E., Lee, N., Rossa, B., Reuter, M., Chaibub Neto, E., & Keshavan, A. (2017). Mindboggling morphometry of human brains. *PLOS Computational Biology*, *13*(2), e1005350. https://doi.org/10.1371/journal.pcbi.1005350

Klein, A., & Tourville, J. (2012). 101 Labeled Brain Images and a Consistent Human Cortical Labeling Protocol . In *Frontiers in Neuroscience* (Vol. 6). https://www.frontiersin.org/articles/10.3389/fnins.2012.00171

Kuo, H.-I., Paulus, W., Batsikadze, G., Jamil, A., Kuo, M.-F., & Nitsche, M. A. (2017). Acute and chronic effects of noradrenergic enhancement on transcranial direct current stimulation-induced neuroplasticity in humans. *The Journal of Physiology*, *595*(4), 1305–1314. https://doi.org/10.1113/JP273137

Leow, L.-A., Marcos, A., Nielsen, E., Sewell, D. K., Ballard, T., Dux, P. E., & Filmer, H. L. (2023). Dopamine alters the effect of brain stimulation on decision-making. *BioRxiv*, 2023.06.05.543812. https://doi.org/10.1101/2023.06.05.543812

Marek, S., Tervo-Clemmens, B., Calabro, F. J., Montez, D. F., Kay, B. P., Hatoum, A. S., Donohue, M. R., Foran, W., Miller, R. L., & Hendrickson, T. J. (2022). Reproducible brain-wide association studies require thousands of individuals. *Nature*, *603*(7902), 654–660.

701 Marques, J. P., Kober, T., Krueger, G., van der Zwaag, W., Van de Moortele, P.-F.,
702 & Gruetter, R. (2010). MP2RAGE, a self bias-field corrected sequence for
703 improved segmentation and T1-mapping at high field. *NeuroImage*, *49*(2),
704 1271–1281. https://doi.org/10.1016/j.neuroimage.2009.10.002

705 Near, J., Ho, Y.-C. L., Sandberg, K., Kumaragamage, C., & Blicher, J. U. (2014).
706 Long-term reproducibility of GABA magnetic resonance spectroscopy.
707 *Neuroimage*, *99*(Supplement C), 191–196.
708 https://doi.org/https://doi.org/10.1016/j.neuroimage.2014.05.059

709 Nitsche, M. A., & Paulus, W. (2000). Excitability changes induced in the human
710 motor cortex by weak transcranial direct current stimulation. *The Journal of*
711 *Physiology*, *527*(3), 633–639. https://doi.org/10.1111/j.1469-7793.2000.t01-1-
712 00633.x

713 Nitsche, Michael A, Lampe, C., Antal, A., Liebetanz, D., Lang, N., Tergau, F., &
714 Paulus, W. (2006). Dopaminergic modulation of long-lasting direct current-
715 induced cortical excitability changes in the human motor cortex. *The European*
716 *Journal of Neuroscience*, *23*(6), 1651–1657. https://doi.org/10.1111/j.1460-
717 9568.2006.04676.x

718 O'Brien, K. R., Kober, T., Hagmann, P., Maeder, P., Marques, J., Lazeyras, F.,
719 Krueger, G., & Roche, A. (2014). Robust T1-weighted structural brain imaging
720 and morphometry at 7T using MP2RAGE. *PloS One*, *9*(6), e99676.
721 https://doi.org/10.1371/journal.pone.0099676

722 Palmer, J., Huk, A. C., & Shadlen, M. N. (2005). The effect of stimulus strength on
723 the speed and accuracy of a perceptual decision. *Journal of Vision*, *5*(5), 376–
724 404. https://doi.org/10.1167/5.5.1

725 Rideaux, R., Ehrhardt, S. E., Wards, Y., Filmer, H. L., Jin, J., Deelchand, D. K.,
726 Marjańska, M., Mattingley, J. B., & Dux, P. E. (2022). On the relationship
727 between GABA+ and glutamate across the brain. *NeuroImage*, *257*, 119273.
728 https://doi.org/https://doi.org/10.1016/j.neuroimage.2022.119273

729 Rideaux, R., Mikkelsen, M., & Edden, R. A. E. (2021). Comparison of methods for
730 spectral alignment and signal modelling of GABA-edited MR spectroscopy data.
731 *NeuroImage*, *232*, 117900.
732 https://doi.org/https://doi.org/10.1016/j.neuroimage.2021.117900

733 Scheenen, T. W. J., Heerschap, A., & Klomp, D. W. J. (2008). Towards 1H-MRSI of
734 the human brain at 7T with slice-selective adiabatic refocusing pulses. *Magma*
735 *(New York, N.Y.)*, *21*(1–2), 95–101. https://doi.org/10.1007/s10334-007-0094-y

736 Sewell, D. K., & Stallman, A. (2020). Modeling the Effect of Speed Emphasis in
737 Probabilistic Category Learning. *Computational Brain and Behavior*, *3*(2), 129–
738 152. https://doi.org/10.1007/S42113-019-00067-6/TABLES/8

739 Stagg, C J, Bachtiar, V., & Johansen-Berg, H. (2011). The role of GABA in human
740 motor learning. *Current Biology*, *21*(6), 480–484.

741 Stagg, Charlotte J, Lin, R. L., Mezue, M., Segerdahl, A., Kong, Y., Xie, J., & Tracey,
742 I. (2013). Widespread modulation of cerebral perfusion induced during and after
743 transcranial direct current stimulation applied to the left dorsolateral prefrontal
744 cortex. *The Journal of Neuroscience : The Official Journal of the Society for*

Neuroscience, *33*(28), 11425–11431. https://doi.org/10.1523/JNEUROSCI.3887-12.2013

Team, J. (2017). *JASP (Version 0.8.3.1)*. https://jasp-stats.org/

Tkáč, I., & Gruetter, R. (2005). Methodology of H NMR Spectroscopy of the Human Brain at Very High Magnetic Fields. *Applied Magnetic Resonance*, *29*(1), 139–157. https://doi.org/10.1007/BF03166960

Vallesi, A., McIntosh, A. R., Crescentini, C., & Stuss, D. T. (2012). fMRI investigation of speed-accuracy strategy switching. *Human Brain Mapping*, *33*(7), 1677–1688. https://doi.org/10.1002/hbm.21312

Watson, A. B., & Pelli, D. G. (1983). Quest: A Bayesian adaptive psychometric method. *Perception & Psychophysics*, *33*(2), 113–120. https://doi.org/10.3758/BF03202828

Wiethoff, S., Hamada, M., & Rothwell, J. C. (2014). Variability in Response to Transcranial Direct Current Stimulation of the Motor Cortex. *BRS*, *7*, 468–475. https://doi.org/10.1016/j.brs.2014.02.003

Wörsching, J., Padberg, F., Helbich, K., Hasan, A., Koch, L., Goerigk, S., Stoecklein, S., Ertl-Wagner, B., & Keeser, D. (2017). Test-retest reliability of prefrontal transcranial Direct Current Stimulation (tDCS) effects on functional MRI connectivity in healthy subjects. *NeuroImage*, *155*, 187–201. https://doi.org/https://doi.org/10.1016/j.neuroimage.2017.04.052

Figure captions

Figure 1: Schematic of the linear ballistic accumulator model.

Figure 2: Example trial. After an initial fixation of 1000ms, a random dot motion (RDM) display was presented for 500ms, then a fixation screen for a further 1300ms. The colour of the fixation dots indicated response instruction: red to focus on accuracy focus, green to speed focus, and orange to balance the two.

Figure 3: Electrode montages and current models for the left prefrontal (A) and SMFC (B) target regions.

Figure 4: Key cortical thickness regions of interest for each of the stimulation conditions: superior frontal (yellow), rostral middle frontal (orange), caudal middle frontal (red), pars triangularis (green), pars opercularis (blue) and precentral (purple) gyri.

Figure 5: locations of the MRS voxels in the frontal and visual cortex (A) and example spectra from the two MRS scan sequences.

Figure 6: Group level effects of instruction on response Caution (top) and discriminability (bottom) for the sham stimulation session.

Figure 7: Group level effects of stimulation to prefrontal cortex (yellow) and SMFC (green) on caution (A, C) and discriminability (B, D) averaged across instruction condition (top) and brown down by instruction condition (bottom).

Figure 8: The ratio of GABA+ to glutamate in the left prefrontal cortex (left) related to how much participants adjusted their response caution with instruction. This was not the case for GABA+/glutamate in the visual cortex (right).

Figure 9: Cortical thickness in left (A) and right (B) rostral middle frontal gyri, and (C) left caudal middle frontal gyrus related to how much participants adjusted their response caution with instruction.

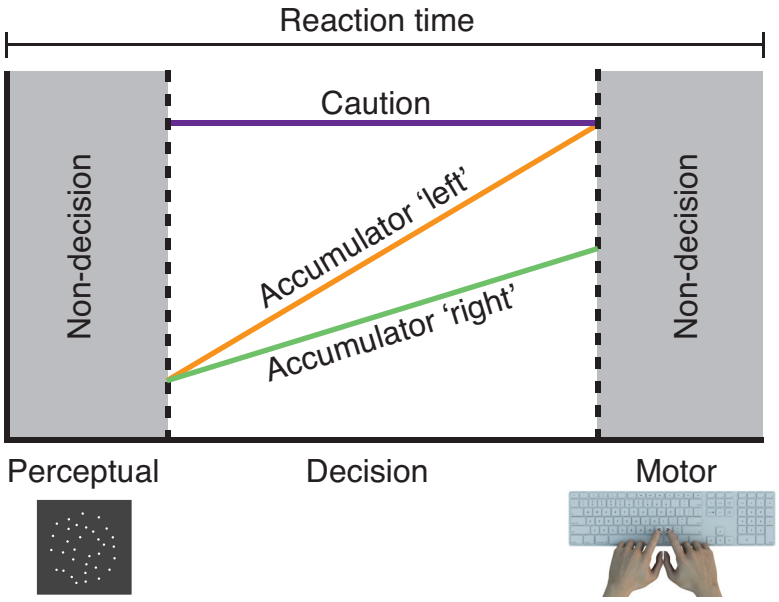

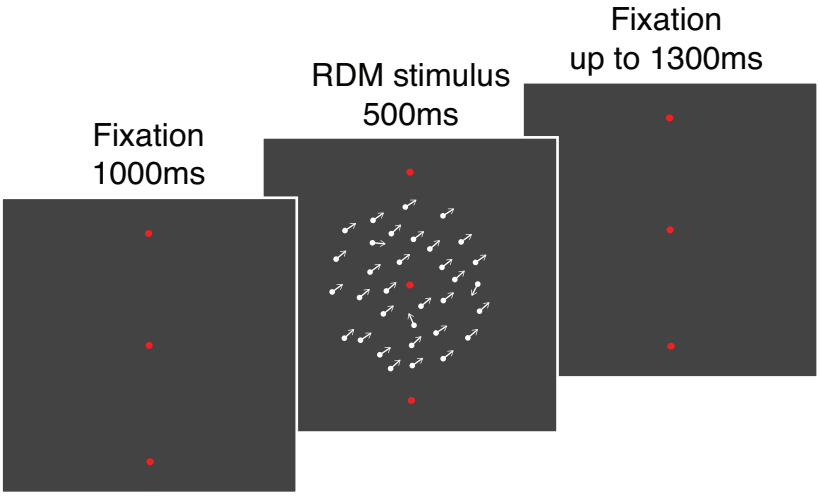

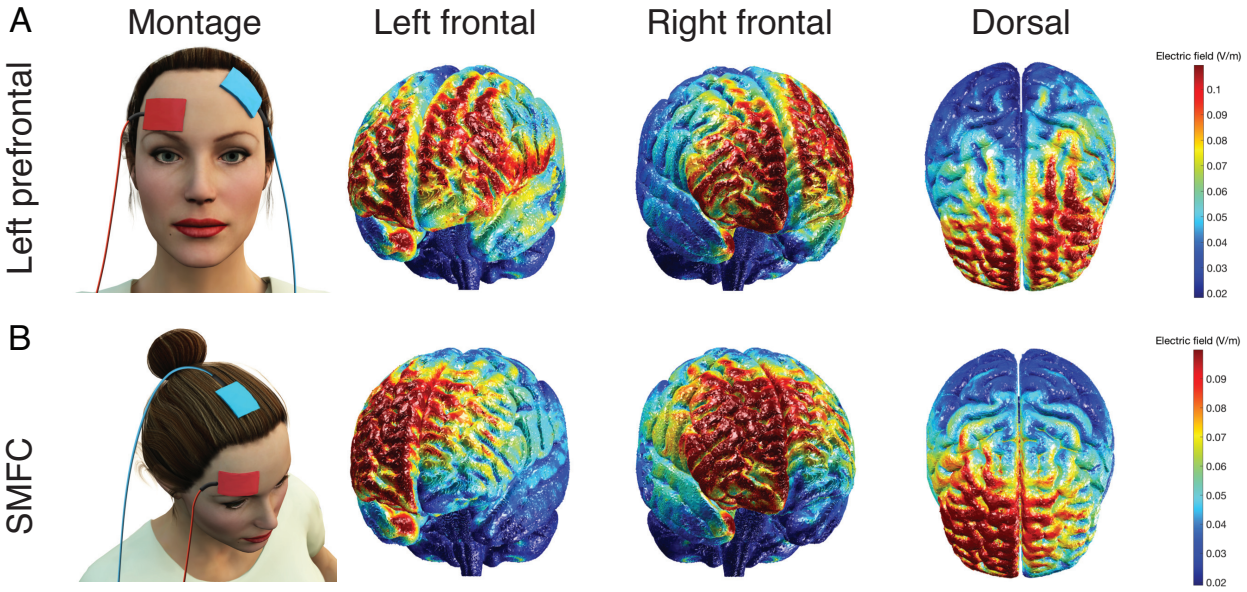

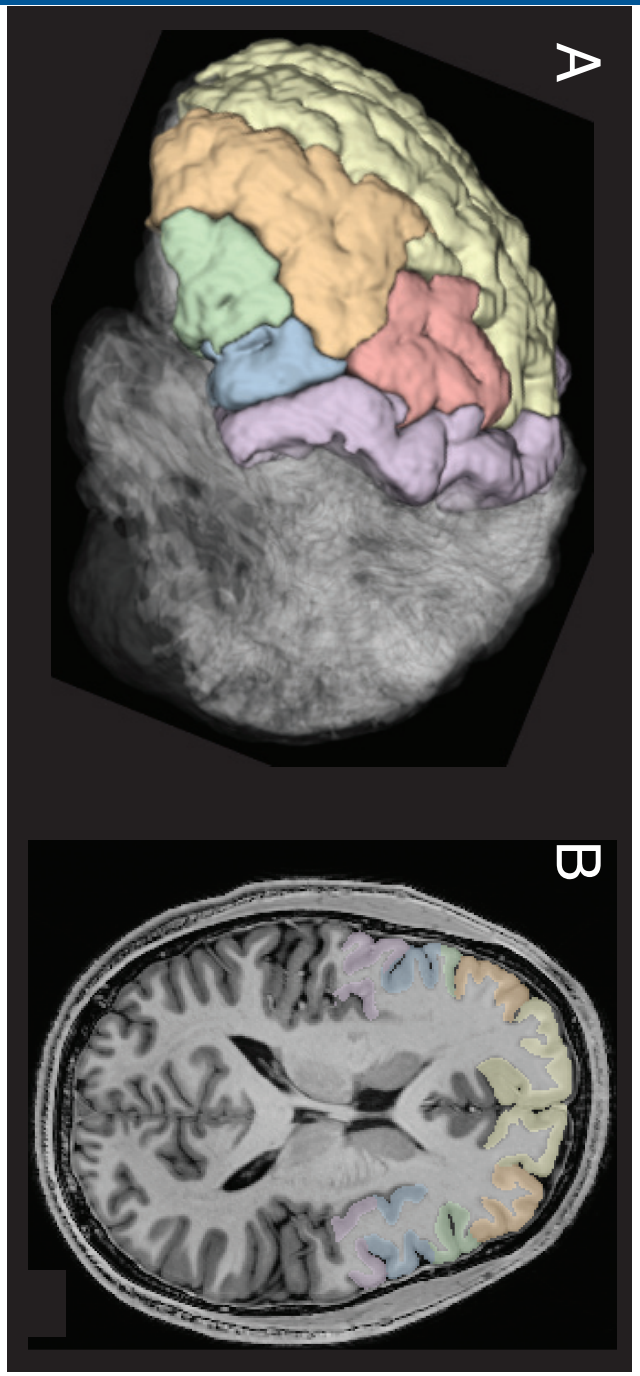

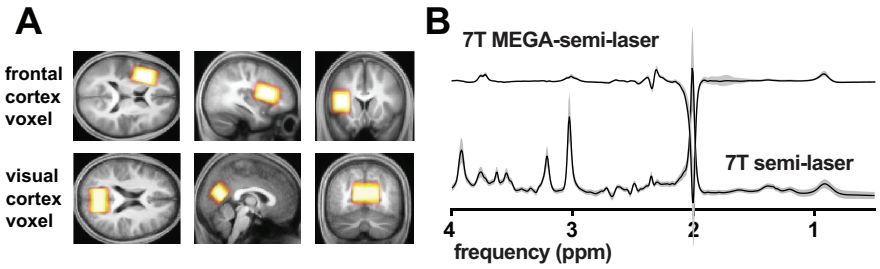

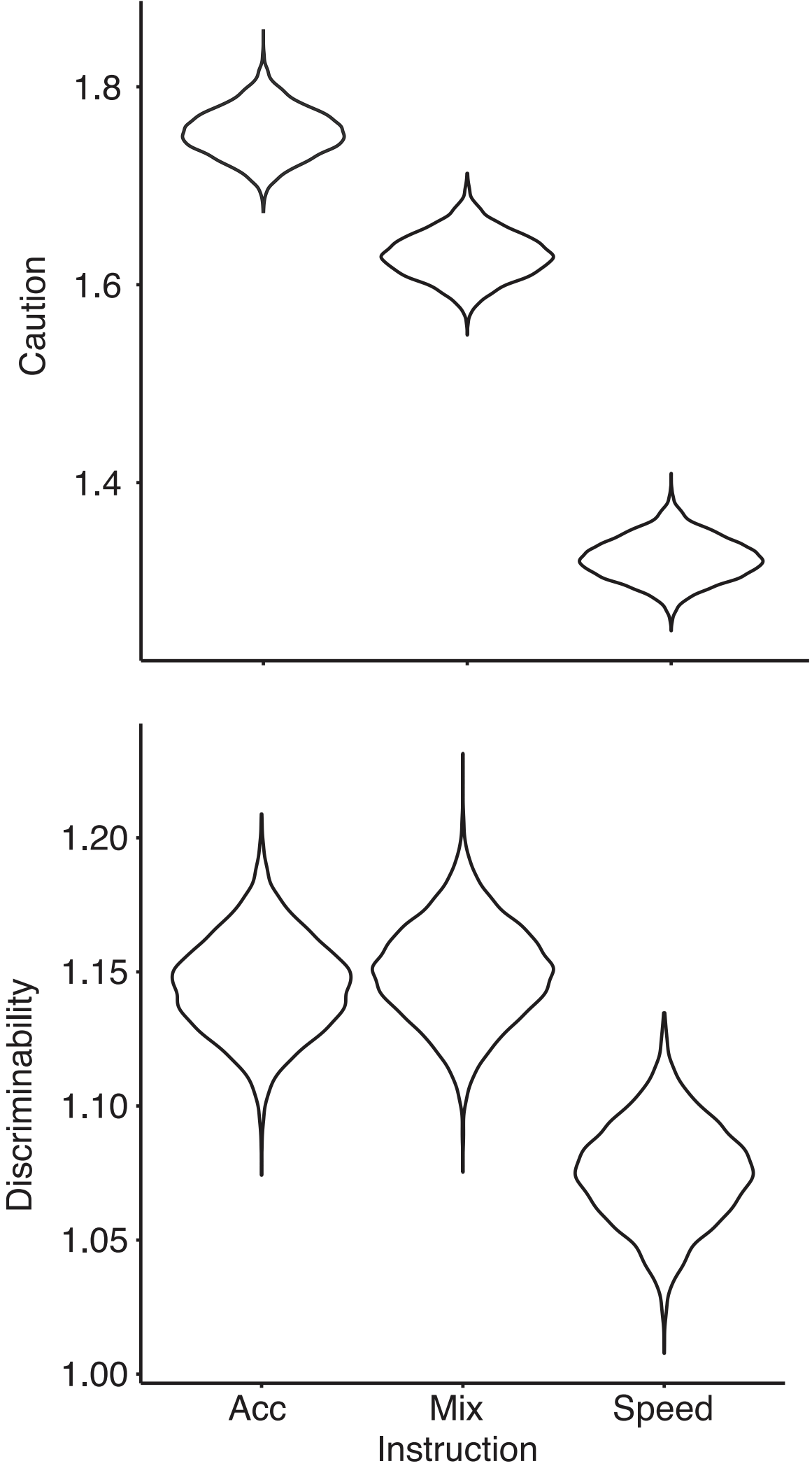

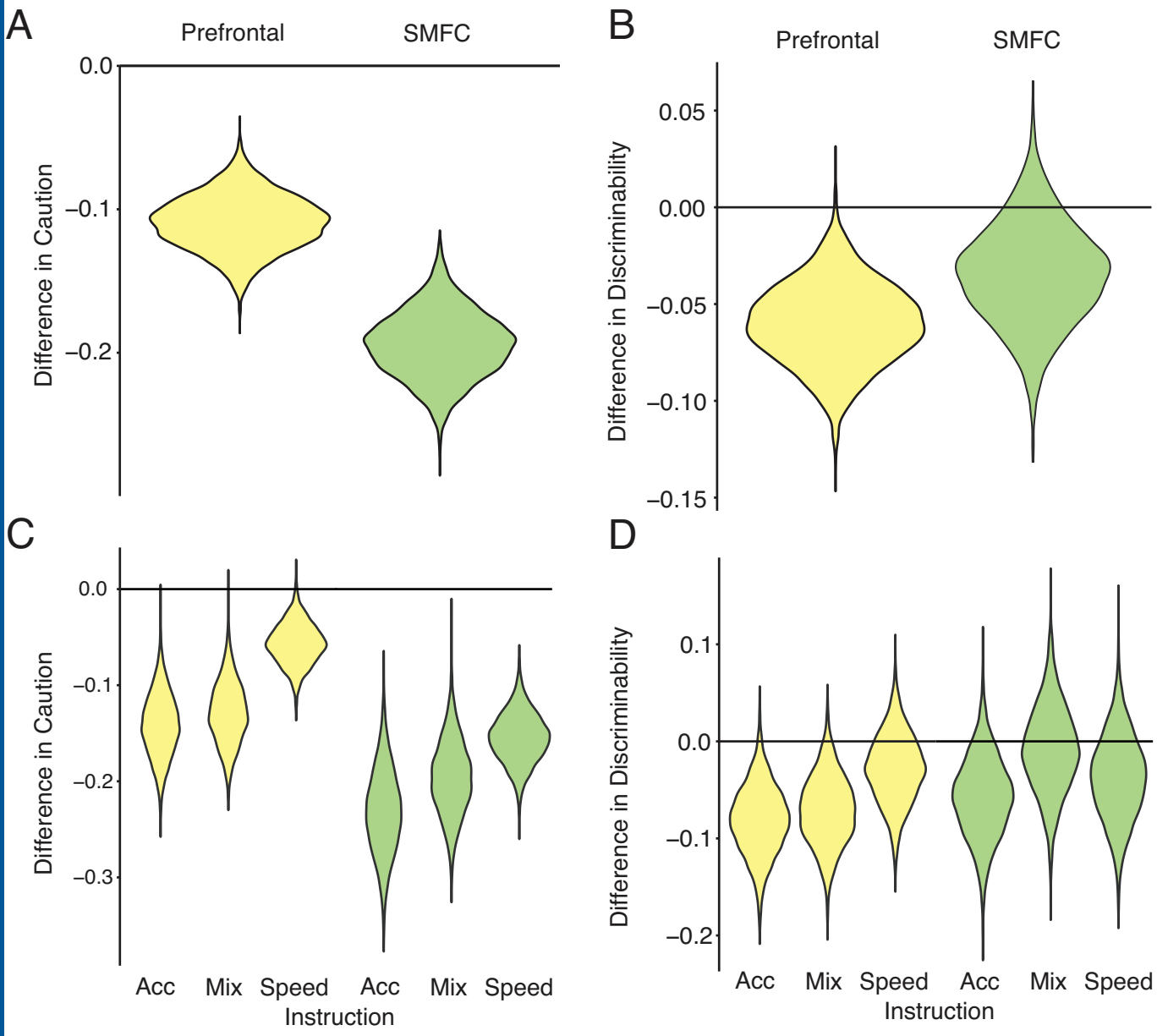

A

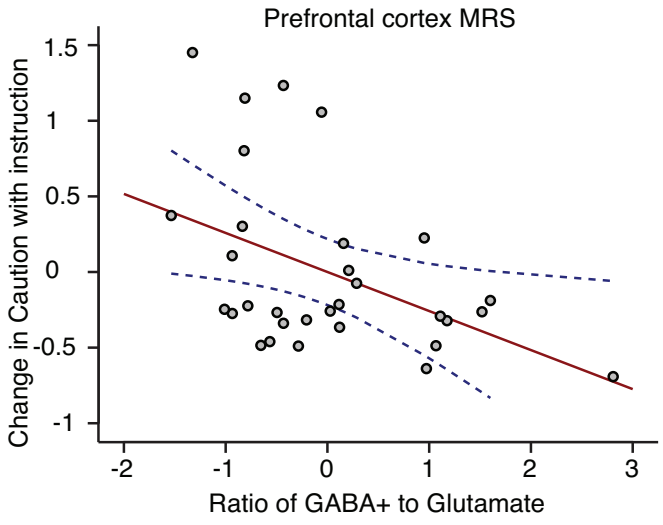

B